The crystal structure of the Y140F mutant of ADP-L-*glycero*-D-*manno*-heptose 6-epimerase bound to ADP-β-D-mannose suggests a one base mechanism

Thomas Kowatz,[1] James P. Morrison,[2] Martin E. Tanner,[2] and James H. Naismith[1]*

[1]Biomolecular Sciences Research Complex, The University of St. Andrews, Fife KY16 9RH, United Kingdom
[2]Department of Chemistry, University of British Columbia, Vancouver, British Columbia V6T 1Z1, Canada

Abstract: Bacteria synthesize a wide array of unusual carbohydrate molecules, which they use in a variety of ways. The carbohydrate L-*glycero*-D-*manno*-heptose is an important component of lipopolysaccharide and is synthesized in a complex series of enzymatic steps. One step involves the epimerization at the C6″ position converting ADP-D-*glycero*-D-*manno*-heptose into ADP-L-*glycero*-D-*manno*-heptose. The enzyme responsible is a member of the short chain dehydrogenase superfamily, known as ADP-L-*glycero*-D-*manno*-heptose 6-epimerase (AGME). The structure of the enzyme was known but the arrangement of the catalytic site with respect to the substrate is unclear. We now report the structure of AGME bound to a substrate mimic, ADP-β-D-mannose, which has the same stereochemical configuration as the substrate. The complex identifies the key residues and allows mechanistic insight into this novel enzyme.

Keywords: LPS biosynthesis; hydride transfer; keto sugar; carbohydrate; SDR enzymes

Introduction

The family of short-chain dehydrogenases/reductases (SDRs) was described in the early 1980s. The first known enzymes of this protein family were an alcohol dehydrogenase from *Drosophila* and a bacterial ribitol dehydrogenase.[1,2] They are 250–350 amino acids long, bind nicotinamide adenine dinucleotide (NAD$^+$) or nicotinamide adenine dinucleotide phosphate (NADP$^+$), and are defined by the catalytic triad Ser (Thr), Tyr, and Lys.[3,4] The proteins catalyze an apparently diverse array of reactions. However, at the chemical centre of each reaction is the stereochemically controlled transfer of a proton and two electrons (hydride) between NAD(P)$^+$ and substrate. For those enzymes that oxidize carbohydrates, normally the Tyr abstracts the proton from a hydroxyl group and hydride is abstracted from the carbon bearing the hydroxyl, forming a keto group. The process works in reverse (keto reduction to hydroxyl) and in many enzymes both the oxidation and reduction steps occur within the same catalytic cycle.

ADP-L-*glycero*-D-*manno*-heptose 6-epimerase (AGME),[5] is a member of the SDR superfamily and catalyzes the interconversion of the stereoisomers ADP-D-*glycero*-D-*manno*-heptose and ADP-L-*glycero*-D-*manno*-heptose. This is the final reaction of the biosynthetic route[6] to the precursor of L-*glycero*-D-*manno*-heptose (L,D-heptose),[7] a component[8] of the core domain of lipopolysaccharide [Fig. 1(a)].[9] Since lipopolysaccharide is involved in maintaining the integrity of the structure of the outer membrane and protecting the
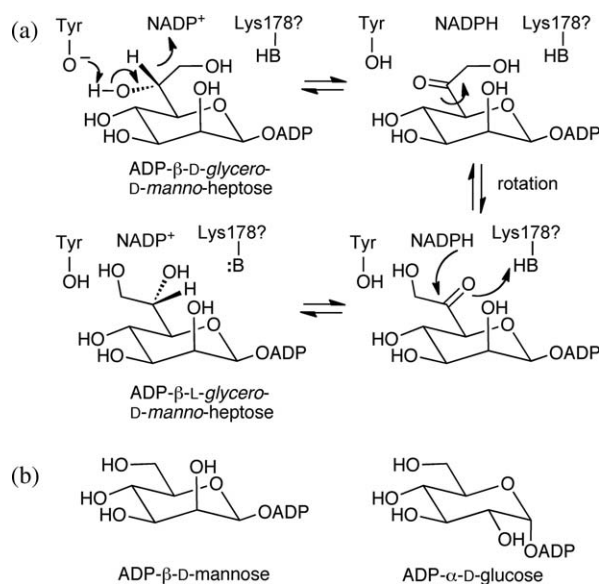
Figure 1. Structures of the heptoses. (a) A two-base mechanism for the interconversion of ADP-β-D-*glycero*-D-*manno*-heptose and ADP-β-L-*glycero*-D-*manno*-heptose, involves oxidation at C6″, followed by rotation around C-5″/C-6″, and then reduction at C-6″. (b) ADP-β-D-mannose (left) is a better mimic of the substrate than ADP-α-D-glucose (right).

organism against destructive intruders, it has long been a target for therapeutic intervention.

AGME preferentially utilizes NADP^{+} but can use NAD^{+} (lower activity)[10] and a chemical mechanism for AGME has been established, which involves transient oxidation of either stereoisomer of ADP-heptose at the C6″ stereogenic centre to form a 6″-keto intermediate[11,12] [Fig. 1(a)], which can then be reduced to either stereoisomer. The crystal structure of AGME with ADP-α-D-glucose bound identified the catalytic site and the "triad" Tyr140, Ser116, and Lys144.[13] The structure left important mechanistic questions open as the glucose moiety of the nucleotide sugar was not well defined in most of the structure and exhibits different orientations. ADP-α-D-glucose differs from the ADP-β-L-*glycero*-D-*manno*-heptose substrate in stereochemistry at C-1″ and at C-2″ [Fig. 1(b)]. Thus though ADP is properly located, the variable sugar ring positions do not allow correct identification of the catalytic residues. Site-directed mutagenesis studies combined with the enzymatic dismutation of ADP-β-D-*manno*-hexodialdose (ADP-β-D-mannose bearing an aldehyde at C-6″) strongly suggested that two acid/base residues were required for activity, Tyr140 (from triad) and Lys178.[14] Release and rebinding of the keto intermediate was excluded by demonstrating that the hydride transfer occurred in an intramolecular fashion.[15] In this mechanism, the first oxidation would occur by hydride transfer to NADP^{+} and Tyr140 would abstract the proton from the hydroxyl. The

C=O of the keto-intermediate would rotate 180° around the C-5″–C-6″ bond allowing reduction from the opposite face and inversion of stereochemistry.[11] Since the oxygen atom would apparently move such a distance, that Tyr140 may no longer function as the acid, Lys178 was proposed donate a proton to the rotated keto group to restore the hydroxyl.[14]

The use of a second acid/base residue other than the Tyr during the hydride transfer is unprecedented. We chose to examine the structural basis of this by determining the crystal structure of AGME with a sugar nucleotide in the β-manno configuration. We now report the complex of Y140F AGME to ADP-β-D-mannose (the C7 hydroxymethyl group of the heptose is replaced by a hydrogen) to 2.35 Å resolution [Fig. 2(a,b)].

Results

### Overall structure

Interestingly our attempts using native protein showed only NADP^{+} (or NADPH) and not ADP-β-mannose bound to the crystals (data not shown). We overcame this problem by cocrystallization of the AGME mutant Y140F (0.08% epimerase activity compared to the wild type[14]) with ADP-β-D-mannose. Unsurprisingly, the mutant protein shares the same fold as wild-type AGME and is found arranged as a pentamer. There is no clear evidence that Cys78, which was found to be oxidized in the previous structure is oxidized here. Our discussion focuses on one monomer from the high-resolution structure, as the 10 monomers within the high-resolution crystal form are essentially identical (average rmsd of 0.06 Å). This monomer is essentially identical to the 20 monomers in the lower resolution form <0.1 Å rmsd), although in one of the 20 subunits (B), we modeled only ADP. In one monomer two residues are missing at the carboxyterminus (amino acids 309 and 310) the other nine subunits lack three residues (amino acids 308–310). No disordered regions have been observed in this structure and there is clear electron density for one molecule of cofactor and one of nucleotide sugar in each of the 10 monomers of AGME Y140F.

The details of the NADP^{+} binding site are almost unchanged from the native structure where they were discussed in detail.[13] There is one slight change, we modeled NADP^{+} with the same amide conformation as seen in other related SDR-enzymes.

Substrate-binding site

In 29 monomers of AGME Y140F, ADP-β-mannose is bound to the active site in the same conformation and in the one subunit with ADP bound, the common atoms overlap. The average atomic temperature factors of ADP-β-mannose (both sugar and nucleotide) are only slightly higher than for the NADP^{+} cofactor
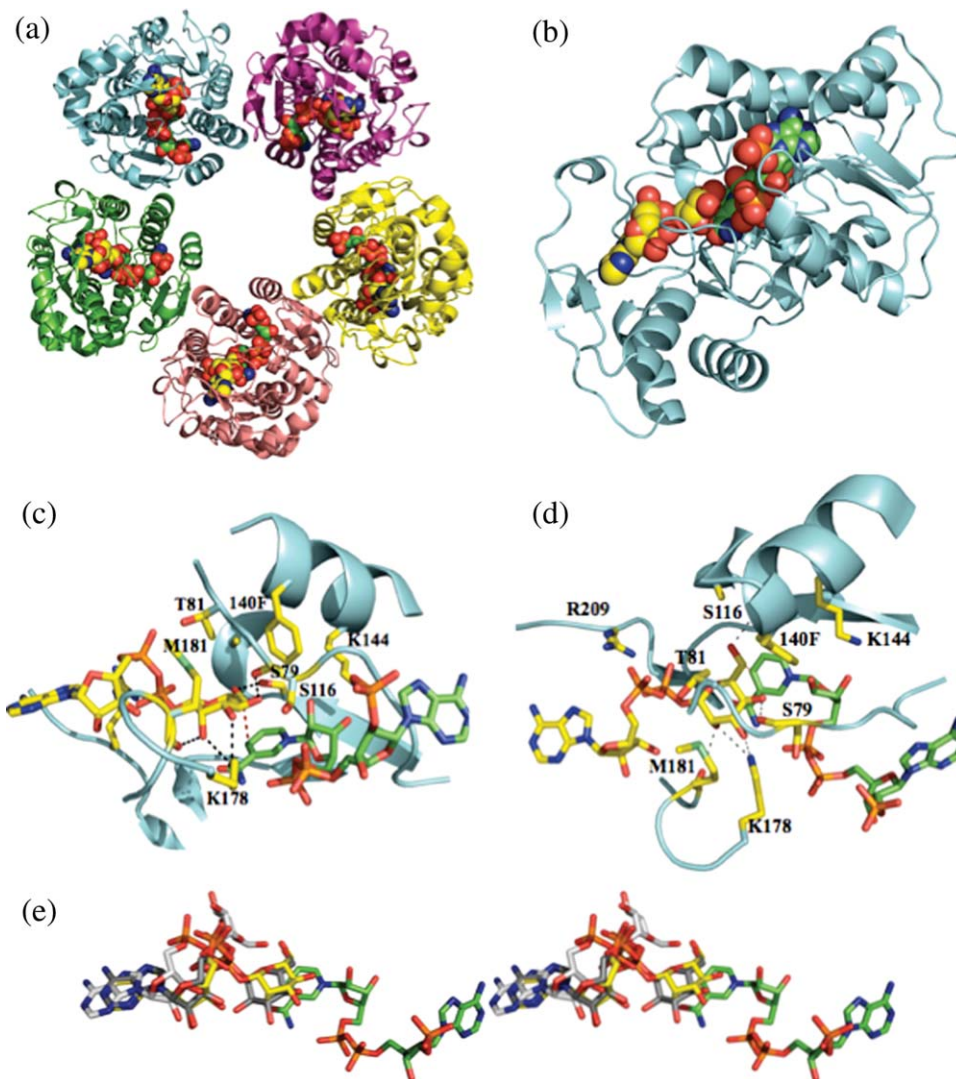
Figure 2. The complex of AGME Y140F with ADP-β-D-mannose. (a) AGME is found as a pentamer and this arrangement as well as the monomer fold is unchanged from previous descriptions. The NADP$^+$ molecule is shown in spacefill with carbons green, whereas ADP-β-D-mannose has carbons colored yellow; oxygen is colored red, nitrogen blue, phosphorous orange. (b) AGME monomer A. The ligands are colored as above. (c) The active site of the AGME Y140F ADP-β-D-mannose complex. The mannose carbohydrate makes extensive hydrogen bond interactions (shown as black dotted lines), consistent with recognition. In the natural protein, the hydroxyl of Tyr140 would hydrogen bond with O6″ of the carbohydrate. Lys178 is located too far from the C6″ atom to transfer protons. The route of hydride transfer is shown as a red dotted line. No other residue is within hydrogen bond distance. (d) The same figures as (c) but rotated by 90°. (e) In the AGME Y140F structure, the carbohydrate ring is oriented differently than seen in either monomer D (carbons colored grey) or monomer B (carbons colored white) in the AGME/ADP-α-D-glucose complex. The ADP groups largely superimpose, the difference is only at the carbohydrate. As the NADP$^+$ groups superimpose they are not shown. [Color figure can be viewed in the online issue, which is available at www.interscience.wiley.com.]

and protein. The adenine moiety of ADP-β-mannose interacts, as described previously.[13] The most significant differences between the bound nucleotide sugars in this mutant ADP-β-mannose structure and the previous wild-type ADP-α-glucose structure lie in the sugar moieties. In ADP-β-mannose the O6″ is hydrogen bonded to the side chain of Ser116 and through a water molecule bridge to O5 [Fig. 2(c,d)]. O4″ hydrogen bonds to O2 of the ribose of NADP$^+$ and to the backbone carbonyl of Ser79 [Fig. 2(c,d)]. O3″ hydrogen bonds to the Ser79 carbonyl and to

the side chain of Lys178. O2″ hydrogen bonds to the side chain of Lys178 and the backbone carbonyl of Met181 [Fig. 2(c,d)]. The recognition of tethered sugars is a complex balance between conformation of the linkage and optimization of hydrogen bond network.[16] The C6″ atom is positioned 2.9 Å from the C4 atom of NADP$^+$ [Fig. 2(c,d); Supporting Information Figure 1]. Comparing the positions of mannose from the AGME Y140F structure and glucose from the previous structure depends on which subunit of the glucose complex is considered. Monomer D of

the previous work is the closest, O6″ and O5″ are positioned similarly and interact with Tyr(Phe)140, Ser116, and Ala118 [Fig. 2(e)]. The other atoms of the sugar occupy different positions [Fig. 2(e)]. The orientation of glucose in monomers B of the ADP-α-glucose AGME complex is completely different and the sugar rings do not overlap [Fig. 2(e)].

Discussion

The C6″ atom of mannose is positioned correctly, both in distance and orientation, for transfer of hydride to C4 of NADP$^+$. The dihedral angle minima adopted by ADP-β-D-mannose are conserved in 29 monomers (one monomer in the lower resolution form only has ADP modeled). This coupled to extensive hydrogen bond recognition between protein and carbohydrate suggest the interaction we observe in the crystal is not an artefact (a known problem with sugar nucleotide proteins[17]). Given the large differences with the ADP-α-glucose, we suggest that the carbohydrate in the ADP-α-glucose/AGME complex was not properly located at the active site residues with respect to substrate. The multiple locations of the glucose ring in the previous complex suggest that the AGME active site is unusually plastic. The new complex provides strong evidence in support of a mechanism involving nonstereospecific oxidation/reduction directly at C-6″.[12] Comparing the structure of AGME Y140F to that of the native structure shows that the side chain of Phe140 superimposes on Tyr140. In devising a mechanism, we made a simple conceptual model in which Phe140 reverts back to Tyr140 (addition of simple hydroxyl) and one of the hydrogen attached to C6″ of ADP-β-mannose is replaced by a hydroxymethyl group (creating the authentic substrate). Our structure indicates that Lys178 is located too far (7.7 Å) from the O6″ of mannose to be involved in proton transfer at O6″. Rotating around the C-5″—C-6″ bond by 120° brings O6″ closer to Lys178 but at 6.2 Å it is still too distant. The 1000-fold reduction in activity of the K178M mutant could be explained by the side chain's hydrogen bonds to O3″ and O2″ of mannose. The additional hydroxymethyl group on the substrate would however clash with the presumed location of the Tyr140 hydroxyl. This clash could be alleviated by either rotating around the C-5″—C-6″ bond of the substrate by 120° (in which case forming a hydrogen bond between O6″ and Tyr140) or by rotating around the Cα—Cβ bond of Tyr140 (which would also lead to formation of a hydrogen bond between O6″ and Tyr140).

The structure supports Tyr140 playing its conventional role of proton abstraction to promote hydride transfer, it is positioned close to the O6″ atom and to Lys144 as would be expected. However, there is no other additional residue that could readily act as an acid/base catalyst. Although a large scale protein conformational change cannot be excluded,
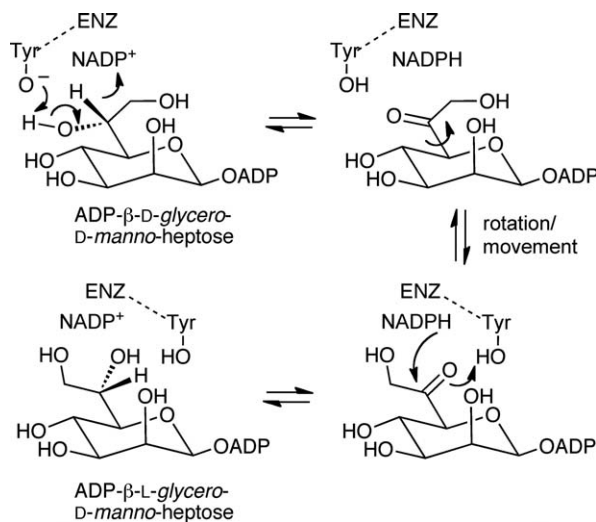
Figure 3. A one base mechanism for the interconversion of ADP-β-D-*glycero*-D-*manno*-heptose and ADP-β-L-*glycero*-D-*manno*-heptose, requires that Tyr140 adjusts its position in response to rotation around the C-5″—C-6″ bond.

this would seem unlikely as the key requirement is always to keep the C6″ atom properly positioned relative to NADP$^+$. Further, since we have crystallized a model of the ternary complex (both nucleotides bound), the potential driving force of such a large change is unclear. If this is so, then the simplest explanation is that Tyr140 acts in both steps (Supporting Information Figure 2a,b). In its current conformation (Cα—Cβ chi angle = 164 °), Tyr140 would abstract the proton from the (R) configuration at C6″ forming the keto intermediate. This keto sugar is now free to rotate 180° around the C-5″—C-6″ bond. This motion would preserve the relative orientations of C6″ and NADP required for hydride transfer and the inversion of stereochemistry. This substrate rotation would essentially put a hydroxymethyl group adjacent to the hydroxyl of Tyr140. To preserve the hydrogen bond to O6″ (and to reduce the clash with the C7″ hydroxymethyl group), Tyr140 would need to rotate by about 30° around the Cα—Cβ bond, to a second position. In position 2 (Cα—Cβ chi angle = 135°) protonated Tyr140 would transfer its proton to O6″ of the keto intermediate, and hydride transfer would generate the (S)-configured epimer (Fig. 3). The structure does not reveal any residues which would block this movement, although it would mean Tyr140 adopting an energetically less favorable conformer. In the reverse reaction, the (S)-configured substrate would initially bind with Tyr140 in position 2, and following oxidation and ketone rotation, Tyr140 would move to position 1 to promote hydride transfer to the opposite face. In this model we have not allowed any movement of the carbohydrate ring or any change in the protein structure (beyond a rotation of the Tyr140 side chain). There will have to be some other small

Table I. *X-ray Data Collection and Refinement Statistics*

Data collection	AGME Y140F	AGME Y140F
λ (Å)	0.954	1.542
Resolution	39–2.35	35–2.8
High-resolution shell (Å)	(2.39–2.35)	(2.85–2.8)
Space group	C2	P2$_1$
Cell (Å, °)	$a = 342.0, b = 60.8, c = 191.8$	$a = 138.1, b = 162.4, c = 185.0$
	$\alpha = \gamma = 90, \beta = 91.4$	$\alpha = \gamma = 90, \beta = 101.4$
Unique reflections	162,824	197,672
Average redundancy	1.9 (1.7)	3.6 (3.5)
I/σ	27 (5.2)	15.3 (1.8)
Completeness (%)	99 (92)	97 (92)
R_{merge}	0.044 (0.192)	0.092 (0.808)
Refinement		
$\quad R_{work}$ (%)	18.6 (23.4)	25.2 (46.7)
$\quad R_{free}$ (%)	20.6 (27.1)	27.2 (49.7)
Number of atoms [average B value (Å^2)]		
$\quad$Protein	24,411 (49)	48,800 (12)
$\quad$Water	1546 (33)	925 (27)
$\quad$NADP$^+$	480 (41)	960 (16)
$\quad$ADP-β-mannose	380 (50)	722 (17)
$\quad$ADP	0	27 (18)
$\quad$Glycerol	60 (51)	0
$\quad$Chloride	2 (61)	0
Average NCS deviations [rmsd (Å)]	0.07	0.08
rmsd bonds (Å)/angles (°)	0.006/1.03	0.013/1.52
Ramachandran favored/disallowed (%)	97.7/0.6	97.4/0.7
Molprobity score (centile)	1.54 (99)	1.67 (100)
PDB code	2x6t	2x86

adjustments to avoid hydrophobic clashes between C7″ of the substrate, and movement of Ser116 would presumably accompany that of Tyr140 to maintain its role in assisting proton abstraction.

The AGME Y140F ADP-β-mannose structure suggests a one-base mechanism is operative for epimerization, consistent with the mechanism of other members of the SDR superfamily. However, the structure does not explain the experimental evidence that was presented in support of a two-base mechanism.[11] A dismutation reaction that converts ADP-β-D-*manno*-hexodialdose (ADP-β-D-mannose bearing an aldehyde at C-6″) into a mixture of ADP-β-D-mannose and ADP-β-D-mannosuronic acid is catalyzed by AGME.[11] When Tyr140 was mutated to Phe, the rate of dismutation only dropped by a factor of five essentially requiring that an alternate base was available to promote hydride transfer.[14] Lys178 was identified as the most likely candidate. It is conceivable that significant conformational changes could occur during the lifetime of the 6″-keto intermediate and reposition the substrate and/or enzyme in an orientation where a second base could participate. Such a dramatic reorientation has been observed in the closely related enzyme UDP-galactose 4-epimerase where the hexose ring undergoes a 180° rotation within the active site during catalysis.[18] Initial structural studies on this enzyme only showed the conformation adopted by UDP-glucose,[19,20] and it was not until the structure of a double mutant bearing bound UDP-galactose was solved that the con-

formational change was visualized.[21] Given these observations, and the observed "plasticity" of the AGME active site seen in the wild-type ADP-α-glucose structure, it would be premature to rule out the two-base mechanism at this time.

The structure of AGME Y140F in complex with ADP-β-mannose, a substrate mimic in the β-*manno* configuration clearly suggests a one base mechanism of AGME. Thus, we provided more insight into the mechanism of this extended short-chain dehydrogenase/reductase which could help in the design of inhibitors against AGME. Further work could also include measurements of their inhibitory potencies and crystal structures of AGME/inhibitor complexes could visualize interactions of inhibitors with this epimerase.

Materials and Methods

Protein expression, purification, and cocrystallization

The *E. coli* strain BL21 (DE3) was transformed with *hldD*-Y140F cloned into the pET-30 Xa/LIC vector (N-terminal 6x His-tag and a Factor Xa cleavage site) (Novagen) for overexpression of the mutated *hldD* gene. The procedure used followed that previously described and employed metal affinity, hydrophobic affinity, and size exclusion. Analysis of enzyme purity was carried out by sodium dodecyl sulfate-polyacrylamide gel electrophoresis and mass spectrometry confirmed integrity and identity. Pure protein was concentrated to 4.1 mg mL^{-1} in 20 m*M*

Tris-HCl, pH 7.5, 50 mM NaCl, 1 mM DTT and ADP-β-D-mannose added to a final concentration of 1 mM. ADP-β-D-mannose was prepared as described previously.[14] The sample was then incubated for 2 h at room temperature before being tested for crystallization. The best crystals were obtained in 1–2 weeks by vapor diffusion of drop (1.5 µl protein + 1.5 µl precipitant) against a reservoir containing 100 µl precipitant (2M (NH$_4$)$_2$SO$_4$, 0.1M HEPES-Na, pH 7.1, 2% PEG 400).

Structure solution and refinement

Before data collection crystals were cryoprotected by immersion in a solution containing 2M ammonium sulfate, 0.1M HEPES-Na, pH 7.1, 2% PEG 400, 2 mM ADP-β-mannose and 15% glycerol for 5 min. Diffraction data were collected at 100 K at a wavelength of 0.954 Å on beamline BM14 at the ESRF, Grenoble. Data from one crystal to 2.35 Å resolution were collected in 0.5° oscillations with a 10 s exposure. Indexing and merging of the data were performed using Denzo and Scalepack in the integrated package HKL2000.[22] The structure was solved by molecular replacement using Molrep.[23] A monomer (monomer A) of the already solved AGME structure (PDB accession code 1EQ2) was used as a search model, all ligands and water molecules were removed prior to search.[13] A solution was found for 10 monomers in the asymmetric unit. Solutions were also found searching with a pentamer. REFMAC5[24] was used to refine the structure and TLS parameters, isotropic B-factors and noncrystallographic symmetry (NCS) restraints were applied throughout. TLS regions were determined using the TLS server as a guide,[25] three regions were chosen, residues, 1–106, 107–198, and 198 to 307. NCS restraints were applied to separately to the three regions. These were restrained to "tight main chain and medium side chain." Manual adjustment including adding ligands was carried out with COOT.[26] Ligands were added to experimental electron density when they were clearly visible in the Fo-Fc map (Supporting Information Figures 3 and 4; Supporting Information Table 1). As each ligand was added it was compared with the others to determine whether the dihedral angles which determine the orientation of the ligand in the protein adopted the same minima. In every case it was unambiguous, the ligands adopt the same dihedral angles. The quality of the electron density does vary between subunits, the Fo-Fc electron density for the nicotinamide and carbohydrate rings were notably weaker than adenosine and phosphate moieties. Both ligands were individually restrained by noncrystallographic symmetry since we decided that the differences from a common minima were unlikely to be functionally significant. One crystallization experiment yielded a different crystal form. This crystal

was frozen prior to data collection and the home source (007HF & SATURN 944 CCD Rigaku) used to collect data. The lower resolution form was solved using a pentameric search model, after rigid body refinement of the monomers, the structure was refined in a similar manner to the high-resolution form (using same TLS regions). Ligands were built into difference electron density, comparing the dihedral angles. In the final stages, the "local" option of REFMAC5.6[24] was used to restrain NCS. Glycerol molecules were modeled in the high-resolution structure but were remote from the active site. The final models were checked and validated using MOLPROBITY.[27] Data and refinement statistics are shown in Table I.

References

1. Persson B, Kallberg Y, Oppermann U, Jörnvall H (2003) Coenzyme-based functional assignments of short-chain dehydrogenases/reductases (SDRs). Chem Biol Interact 143–144:271–278.
2. Jornvall H, Persson M, Jeffery J (1981) Alcohol and polyol dehydrogenases are both divided into two protein types, and structural properties cross-relate the different enzyme activities within each type. Proc Natl Acad Sci USA 78:4226–4230.
3. Oppermann U, Filling C, Hult M, Shafqat N, Wu X, Lindh M, Shafqat J, Nordling E, Kallberg Y, Persson B, Jornvall H (2003) Short-chain dehydrogenases/reductases (SDR): the 2002 update. Chem Biol Interact 143–144:247–253.
4. Filling C, Berndt KD, Benach J, et al. (2002) Critical residues for structure and catalysis in short-chain dehydrogenases/reductases. J Biol Chem 277:25677–25684.
5. Pegues JC, Chen LS, Gordon AW, Ding L, Coleman WGJ (1990) Cloning, expression, and characterization of the *Escherichia coli* K-12 rfaD gene. J Bacteriol 172:4652–4660.
6. Kneidinger B, Marolda C, Graninger M, Zamyatina A, McArthur F, Kosma P, Valvano MA, Messner P (2002) Biosynthesis pathway of ADP-L-glycero-beta-D-mannoheptose in *Escherichia coli*. J Bacteriol 184:363–369.
7. Coleman WGJ (1983) The rfaD gene codes for ADP-L-glycero-D-mannoheptose-6-epimerase. An enzyme required for lipopolysaccharide core biosynthesis. J Biol Chem 258:1985–1990.
8. Adams GA, Quadling C, Perry MB (1967) D-Glycero-D-manno-heptose as a component of lipopolysaccharides from Gram-negative bacteria. Can J Microbiol 13:1605–1613.
9. Raetz CRH (1990) Biochemistry of endotoxins. Annu Rev Biochem 59:129–170.
10. Ni Y, McPhie P, Deacon A, Ealick S, Coleman WG, Jr (2001) Evidence that NADP+ is the physiological cofactor of ADP-L-glycero-D-mannoheptose 6-epimerase. J Biol Chem 276:27329–27334.
11. Morrison JP, Read JA, Coleman WG, Jr, Tanner ME (2005) Dismutase activity of ADP-L-glycero-D-mannoheptose 6-epimerase: evidence for a direct oxidation/reduction mechanism. Biochemistry 44:5907–5915.
12. Read JA, Ahmed RA, Morrison JP, Coleman WGJ, Tanner ME (2004) The mechanism of the reaction catalyzed by ADP-beta-L-glycero-D-manno-heptose 6-epimerase. J Am Chem Soc 126:8878–8879.

13. Deacon AM, Ni YS, Coleman WG, Jr, Ealick SE (2000) The crystal structure of ADP-L-glycero-D-mannoheptose 6-epimerase: catalysis with a twist. Structure 8:453–462.
14. Morrison JP, Tanner ME (2007) A two-base mechanism for *Escherichia coli* ADP-L-glycero-D-manno-heptose 6-epimerase. Biochemistry 46:3916–3924.
15. Mayer A, Tanner ME (2007) Intermediate release by ADP-L-glycero-D-manno-heptose 6-epimerase. Biochemistry 46:6149–6155.
16. Bryce RA, Hillier IH, Naismith JH (2001) Carbohydrate-protein recognition: molecular dynamics simulations and free energy analysis of oligosaccharide binding to concanavalin A. Biophys J 81:1373–1388.
17. Steiner K, Hagelueken G, Messner P, Schaffer C, Naismith JH (2010) Structural basis of substrate binding in WsaF, a rhamnosyltransferase from *Geobacillus stearothermophilus*. J Mol Biol 397:436–447.
18. Frey PA (1996) The Leloir pathway: a mechanistic imperative for three enzymes to change the stereochemical configuration of a single carbon in galactose. FASEB J 10:461–470.
19. Liu Y, Thoden JB, Kim J, et al. (1997) Mechanistic roles of tyrosine 149 and serine 124 in UDP-galactose 4-epimerase from *Escherichia coli*. Biochemistry 36:10675–10684.
20. Thoden JB, Hegeman AD, Wesenberg G, Chapeau MC, Frey PA, Holden HM (1997) Structural analysis of UDP-sugar binding to UDP-galactose 4-epimerase from *Escherichia coli*. Biochemistry 36:6294–6304.
21. Thoden JB, Holden HM (1998) Dramatic differences in the binding of UDP-galactose and UDP-glucose to UDP-galactose 4-epimerase from *Escherichia coli*. Biochemistry 37:11469–11477.
22. Minor W, Cymborowski M, Otwinowski Z (2002) Automatic system for crystallographic data collection and analysis. Acta Phys Polon A 101:613–619.
23. Vagin A, Teplyakov A (1997) MOLREP: an automated program for molecular replacement. J Appl Cryst 30:1022–1025.
24. Murshudov GN, Vagin AA, Lebedev A, Wilson KS, Dodson EJ (1999) Efficient anisotropic refinement of macromolecular structures using FFT. Acta Cryst D 55:247–255.
25. Painter J, Merritt EA (2006) Optimal description of a protein structure in terms of multiple groups undergoing TLS motion. Acta Cryst D 62:439–450.
26. Emsley P, Cowtan K (2004) Coot: model-building tools for molecular graphics. Acta Cryst D 60:2126–2132.
27. Davis IW, Leaver-Fay A, Chen VB, Block JN, Kapral GJ, Wang X, Murray LW, Arendall WB 3rd, Snoeyink J, Richardson JS, Richardson DC (2007) MolProbity: all-atom contacts and structure validation for proteins and nucleic acids. Nucleic Acids Res 35:W375–W383.